Use of a Genetic Algorithm in Modelling Small Structures in Airframes

Characterising and modelling joints, seams, and apertures

R Xia, J F Dawson, I D Flintoft, A C Marvin, S J Porter
Department of Electronics
University of York
York, UK
jfd1@ohm.york.ac.uk

***Abstract*—In this paper, a Genetic Algorithm (GA) is used to build macro models of small structures, such as joints and apertures, for use in large-scale computer simulations for aircraft electromagnetic compatibility (EMC) testing and certification. The field penetrating the structure is approximated by radiated fields of electric and magnetic dipole moment array. A GA is applied to determine the dipole moment array that produces the same effect as the structure that is to be built into the model. A scanning frame and a magnetic field probe have been constructed to measure the fields in the vicinity of the small structure, to provide field data for the fitting process.**

Keywords-EMC testing; macro model; genetic algorithm; near-field measurement;

I. INTRODUCTION

The HIRF-SE project is an EU Framework 7 project that aims to provide a computational framework which can be used for aircraft EMC prediction to provide data for EMC certification and testing. Macro models of small structures, such as panel joints, that are too small to be built into a detailed aircraft model without excessive computational requirements are being considered by the University of York.

Our previous paper [1] investigates the method of field transformations, while in this paper the application of a GA is discussed as another approach. The GA is an 'evolutionary' computational method that is widely used as an optimization tool. Like evolution in nature, there are parameters that affect the process such as 'crossover', 'mutation' and 'migration' which makes the GA tunable to fit a particular optimization problem.

The modeling work here uses a GA to search for an optimal source that can reproduce the same effect as the field that penetrates in the structure being modeled. The source can be included in numerical electromagnetic modelling techniques to simulate the effect of field coupling through small structures if the source is coupled to the fields incident on the opposite side of the structure, via a frequency-dependent transfer function.

II. COMPUTATIONAL METHOD

A. Dipole Moment Approach

Figure 1 shows how the electric field penetrates an aperture in a conductive sheet. Providing the slot is electrically small, the penetrating field can be approximated by the fields of electric or magnetic dipoles placed on the surface of the conductive sheet [2].

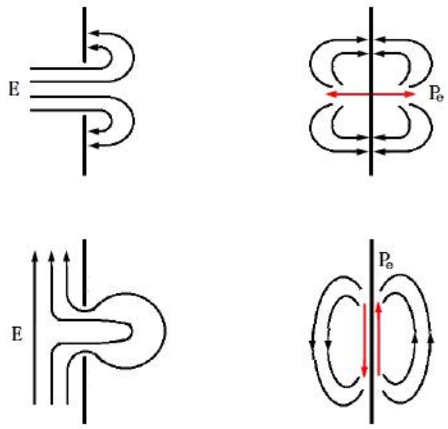

Figure 1 Representation of penetrating fields by dipole moments, reproduced based on Figure 4.31 in [2]

The equivalent dipole moments are infinitesimal in size, and the polarization current can be calculated from aperture size, incident field and polarisability of the aperture, where for the equivalent electric dipole moment:

$$\overline{P}_e = \varepsilon_0 \alpha_e \hat{n} E_n \delta(x - x_0)\delta(y - y_0)\delta(z - z_0) \qquad (1)$$

The α_e term is the polarisability and varies with the size and shape of the aperture. McDonald [3] and [4] gives approximations to the electric and magnetic polarisabilities of apertures of a number of shapes. The structure being modeled here is an electrically small slot being illuminated by an electric field polarized across its width. It can be replaced by the dipole moments of the three dominant fields as shown in *Figure 2*.

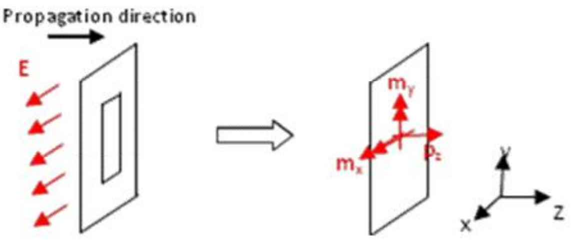

Figure 2 Replacement of slot by three dominant dipole moments

B. Use of a GA to find the equivalent Dipole Moment

The GA provided by MATLAB [7] is used in our approach. A population size of 50 is used with a search bounded by limits given below. 300 generations are run, and the mutation function is set as "adaptive feasible", which ensures that mutated members of the population lie within the bounded search volume.

The design variable for the GA is the equivalent current flows on the dipole moment. The dipole moment can be written as a function of current as $p = \frac{I_e dl}{j\omega}$ for electric dipole moment, and $m = \frac{I_m dl}{j\omega}$ for magnetic dipole moment. Where I_e and I_m are equivalent electric and magnetic currents respectively, *dl* is the size of the dipole, and ω is the angular frequency of the current.

For the GA to operate efficiently, it is important to set the search bound accurately. A simple estimation of the polarization current magnitude is used to set the search bound. The estimation here is based on the radiated electric field of an electric dipole [5]:

$$E_\theta = j\frac{Z_0 I dl k}{4\pi r}\left\{1 - \frac{1}{k^2 r^2} + \frac{1}{jkr}\right\}e^{-jkr}\sin\theta \qquad (2)$$

where the symbols have their usual meanings. Taking the magnitude of the complex terms, the expression can be reduced to

$$|E_\theta| = 30\frac{dlk}{r}\left\{\left|1 - \frac{1}{k^2 r^2} + \frac{1}{jkr}\right|\right\}I \qquad (3)$$

From a measured electric field, $E_{\theta m}$, an upper bound on the dipole current I_{max} can be estimated as

$$I_{\max} = \frac{E_{\theta m}}{30\frac{dlk}{r}\left\{\left|1 - \frac{1}{k^2 r^2} - j\frac{1}{kr}\right|\right\}}D \qquad (4)$$

To estimate maximum possible dipole current, the $E_{\theta m}$ here is the maximum electric field in the measurement surface and r is the distance of the furthest observation point. Furthermore, a scaling factor D is used to expand the search bound in order to compensate errors of the above estimation. In the following test cases, D is set to 2.

This work was partly funded under the EU Framework 7 programme contract number: 205294 (FP7) as part of the HIRF-SE project.

To test the operation of GA with the parameters defined above, the GA is used to find the polarization current on two identical dipoles of 3mm in size, placed 15cm apart. The radiated field is calculated using a full-field expression given in [6] with the dipole currents being in phase and set at 7.96μA at 2GHz. The cost function is the sum of the mean decibel errors of the three field components between the calculated radiated field and that calculated from the polarization currents found by the GA.

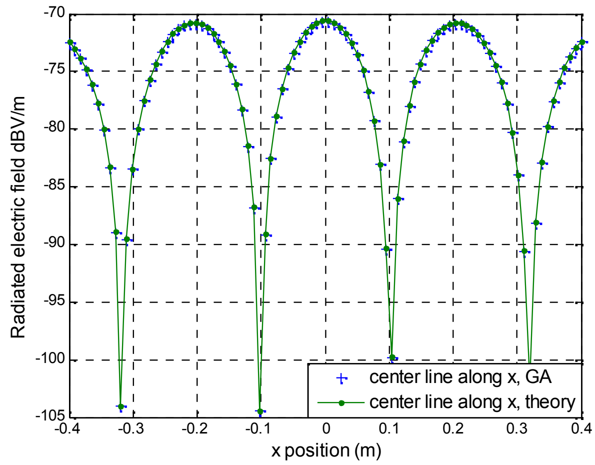

(a)

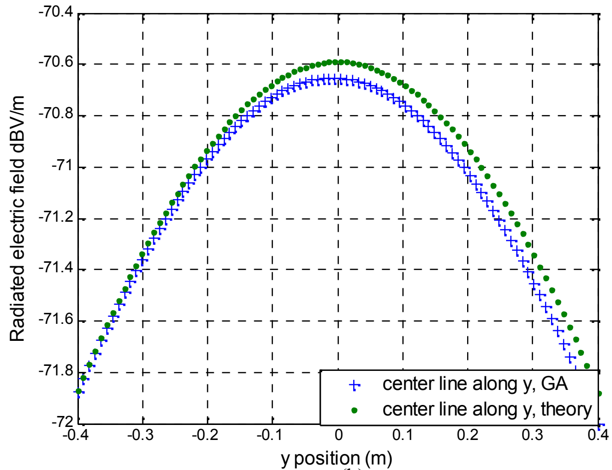

(b)

Figure 3 Simulation result of fitting polarization current on dipoles using GA (a): H-plane cut, (b): E-plane cut

The error in the x-oriented field component is:

$$C_x = \frac{20}{N_x N_y}\sum_{n_y=1}^{N_y}\sum_{n_x=1}^{N_x}\{|\log_{10}(|E_{GA}|) - \log_{10}(|E_{mea}|)|\} \quad (5)$$

The overall error is therefore:

$$C = C_x + C_y + C_z \qquad (6)$$

Where N_x and N_y are the number of points along x and y-axis on the observation surface. E_{GA} and E_{mea} represent the radiated electric fields produced by the dipole moment from GA and that (measured or) calculated. The decibel value is taken to ensure that the curve fit is good for small field values as well as large ones.

The radiated field is taken on a planar surface 30cm from the dipole pair. *Figure 3* shows the calculated electric field and that reproduced using the excitation found by GA. Two plane cuts are shown here, where x is perpendicular to the direction of polarization, and y is parallel to the polarization direction

III. MEASUREMENT METHOD

A. *Magnetic Field Probe*

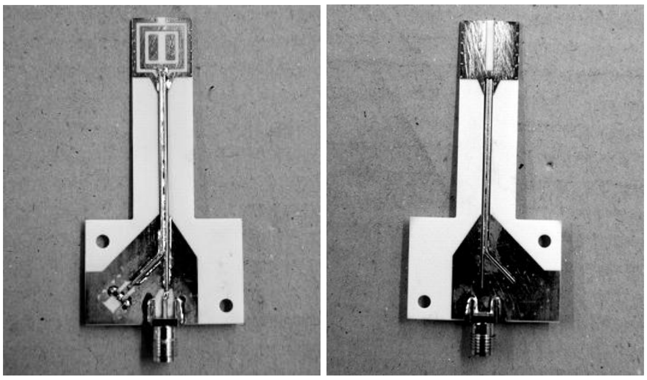

Figure 4 Loop antenna built as magnetic field probe

A magnetic field probe loop was fabricated on a microwave PCB laminate (Fig. 4). An outer loop with a gap acts as a shield against electric field pickup. Two rectangular copper plates are placed to provide further shielding against electric field on the loop side whilst a slotted ground-plane is used below the loop. The probe is terminated through two semi-rigid cables. One of those is mounted to an SMA connector, and another terminated by a 50 ohms load, which is formed by two 100 ohms surface-mount resistors, connected in parallel to reduce stray inductance.

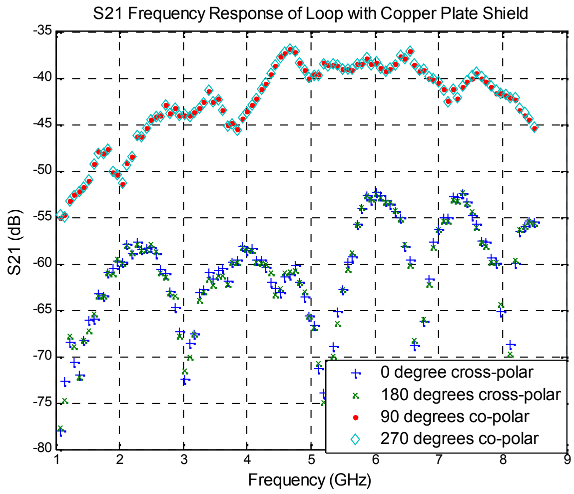

Figure 5 Co-polar and cross-polar measurement of the loop in an anechoic chamber

Figure 5 shows the co-polar and cross-polar measurement of the loop in an anechoic chamber. 0 degrees is defined as the direction of polarization of the incident electric field and is parallel to the loop. It can be seen that the co-polar response is at least 10dB higher than that of the cross-polar response between 2GHz and 8.5GHz.

Since the loop is used to measure magnetic field, the antenna factor of the loop is defined as the ratio of incident magnetic field to load voltage. In the far-field region, $|E| = |H| \times \eta_0$, where η_0 is the impedance of free space. The antenna factor of the loop can then be written as:

$$AF_{loop} = \frac{H_{inc}}{V_{load}} = \frac{E_{inc}}{\eta_0 V_{load}} \quad (5)$$

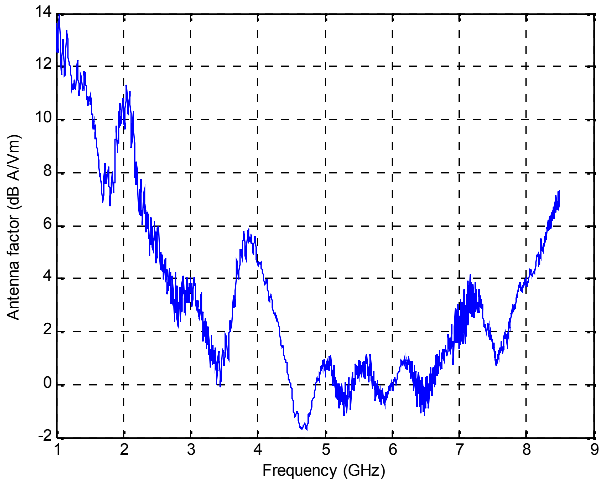

Figure 6 Antenna factor of the loop

B. *Measurement Using Scaning Frame*

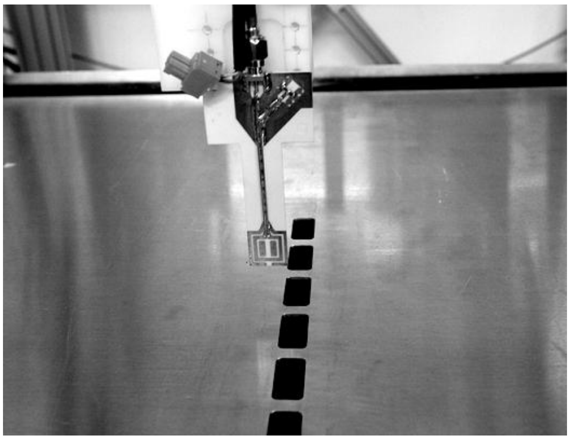

Figure 7 Scanning fields penetrating the slot panel

The loop antenna was then used to measure the field penetrating an array of slots. The slot array consists of six 2cm long x 1cm wide slots separated by 5mm, cut into a 2mm thick aluminum sheet. The loop was mounted to a scanner, which used stepper motors to drive the loop to scan a plane above the structure.

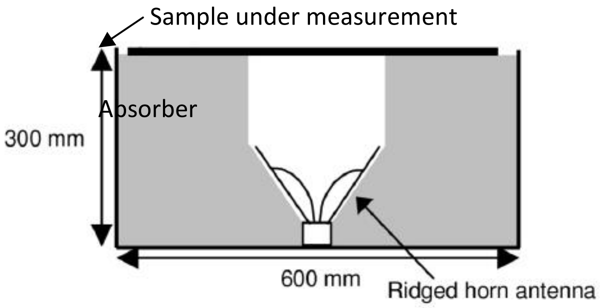

Figure 8 Geometry of absorber box

An absorber box [8] was used to produce an environment close to frees-pace by illuminating the sample being measured through a hole cut in absorbers. It saves time and cost on the edge treatment compared to a dual anechoic chamber measurement, and reduces the space required by the measurement facility.

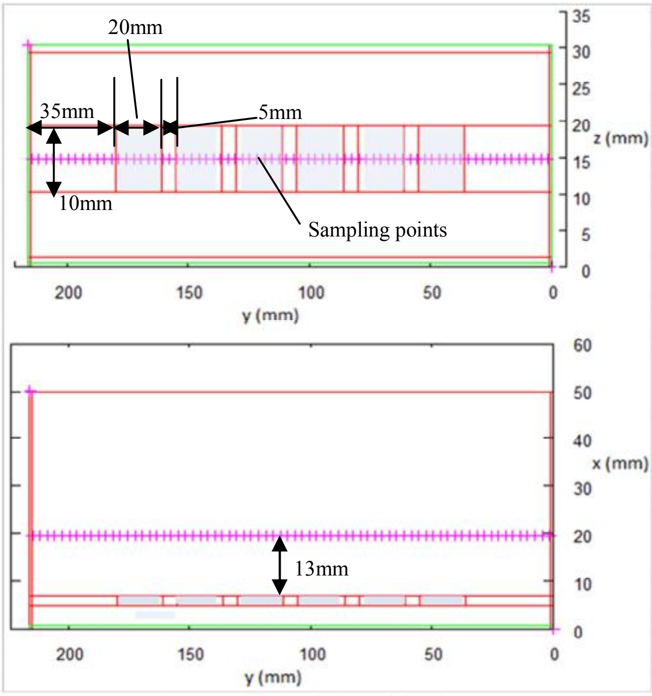

Figure 9 TLM simulation of the slot array

A TLM model of the slot structure was constructed to provide comparison with the measurement. The longitudinal magnetic field was recorded 13mm from the slot, which is the same as the measurement height in *Figure 7*.

Figure 11 shows measurement result compared to that from the TLM simulation. The excitation in TLM was a plane wave of 1V/m z-polarized electric field, while that in the measurement was a horn antenna placed in a cavity surrounded by absorber. The absolute magnetic fields cannot be compared, as the excitations are different.

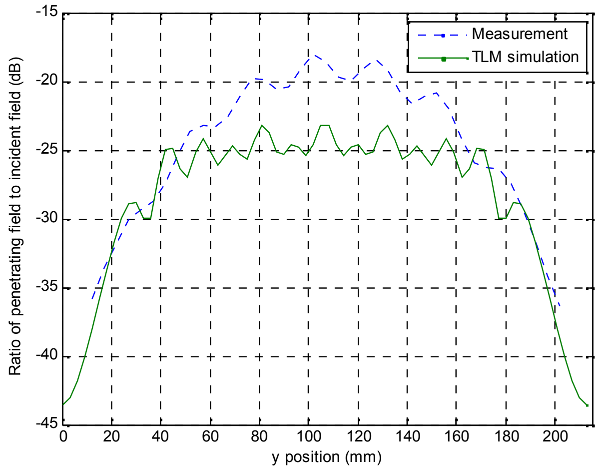

Figure 10 Ratio of penetrating magnetic field to incident field in measurement and TLM simulation

IV. Results

A. *Use of the GA to fit measured near-field dipole moments*

In this section, the GA is used to reproduce the source using measurement data. The measurement was taken on the same slot array structure described Section III(b), which was also presented in a previous paper on this project [1].

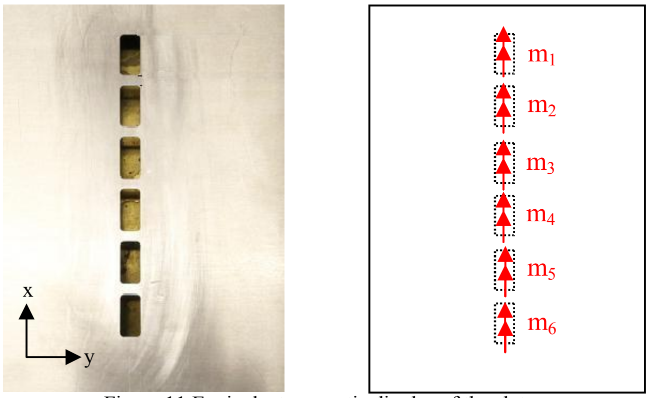

Figure 11 Equivalent magnetic dipoles of the slot array

Since only y-polarized electric field was measured, the cost function is modified so that the GA fits only E_y in the measurement. The source is then constructed as 6 electric dipole moments, placed at the centers of the slots as shown in *Figure12*.

The GA is set to run for 1000 generations, each with a population size of 50. ‘Adaptive feasible’ is used as the mutation function. The results are plotted in *Figures 13* and *14* below.

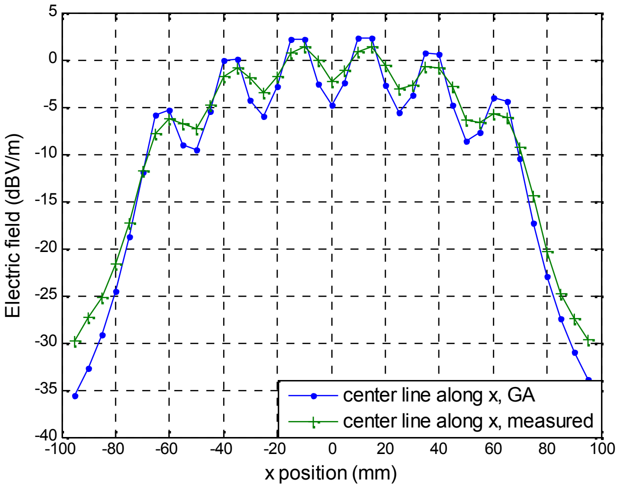

Figure 12 X-axis cut of electric field produced by GA and measurement

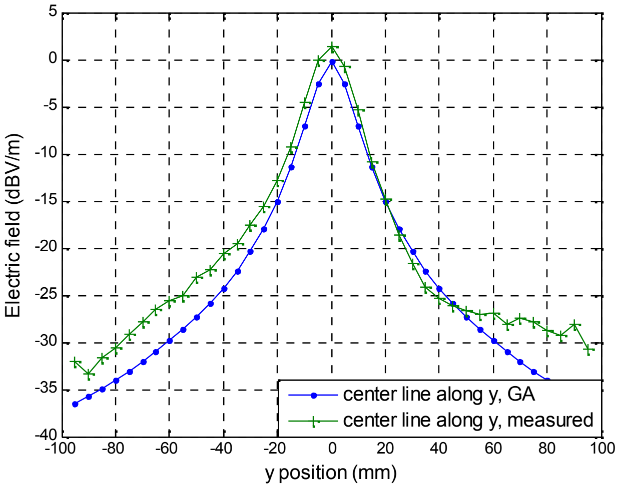

Figure 13 Y-axis cut of electric field produced by GA and measurement

Figure 13 and *14* shows the dipole moments that the GA found can produce electric field follows the shape of that from measurement. In the measurement, the slots are so close that there is mutual coupling between them, which is not accounted in the field produced by the dipole moments. In addition, the measured field is averaged across the reception aperture of the measurement probe, while the field produced by the dipole moments is calculated at the exact location of the measuring point. It is considered the results can be improved by increasing the density of the dipole moments and properly considering the averaging of the field produced by antenna physical size.

V. SUMMARY

In this paper, a GA has been shown to be capable of finding the magnitude of an equivalent radiating source based on simulation or measurement data. The specific goal of our modeling work is to reproduce the radiated field, so it is necessary to create an equivalent source that can produce a similar effect to the original source, rather than exactly re-creating the original source itself..

ACKNOWLEDGMENT

The authors would like to thank A White, A Patterson, J Emery, and M Hough, who fabricated the scanner hardware, and G Short who developed the scanner control and data acquisition software.

REFERENCES

[1] R. Xia, J. F. Dawson, I. D. Flintoft, A. C. Marvin and S. J. Porter, ‘Building Marcro Models for Small Structures on Airframe’, EMC Europe, 2011.

[2] D. M. Pozar, ‘Microwave Engineering 2nd Edition’. John Wiley & Sons, Inc.,1998. pp238.

[3] N. A. McDonald, “Polynomial Approximations for the Transverse Magnetic Polarizabilities of Some Small Apertures,” Microwave Theory and Techiniques, IEEE Transactions on, vol. 35, 1987, pp. 20-23.

[4] N.A. McDonald, “Simple Approximations for the Longitudinal Magnetic Polarizabilities of Some Small Apertures,” ,” Microwave Theory and Techiniques, IEEE Transactions on, vol. 36, 1988, pp. 1141-1144.

[5] C. A. Balanis, ‘Antenna Theory, Analysis and Design 2nd Edition’. John Wiley & Sons, Inc.,1997. pp135.

[6] J. D. Jackson, ‘Classical Electromagnetics 3rd Edition’, . John Wiley & Sons, Inc., 1999, pp411.

[7] Mathworks, Product R2012a Documentation: ga, available at: http://www.mathworks.co.uk/help/toolbox/gads/ga.html , Accessed 1 March 2012.

[8] A. C. Marvin, L. Dawson, I. D. Flintoft and J. F. Dawson, A Method for the Measurement of Shielding Effectiveness of Planar Samples Requiring no Sample Edge Preparation or Contact, IEEE Transactions on Electromagnetic Compatibility, Vol. 51, No. 2, April 2009.

Xia, R.; Dawson, J.F.; Flintoft, I.D.; Marvin, A.C.; Porter, S.J., "Use of a Genetic Algorithm in modelling small structures in airframes: Characterising and modelling joints, seams, and apertures," Electromagnetic Compatibility (EMC EUROPE), 2012 International Symposium on , vol., no., pp.1,5, 17-21 Sept. 2012
doi: 10.1109/EMCEurope.2012.6396718
URL: http://ieeexplore.ieee.org/stamp/stamp.jsp?tp=&arnumber=6396718&isnumber=6396647